nature medicine

A SARS-like cluster of circulating bat coronaviruses shows potential for human emergence

Vineet D Menachery[1], Boyd L Yount Jr[1], Kari Debbink[1,2], Sudhakar Agnihothram[3], Lisa E Gralinski[1], Jessica A Plante[1], Rachel L Graham[1], Trevor Scobey[1], Xing-Yi Ge[4], Eric F Donaldson[1], Scott H Randell[5,6], Antonio Lanzavecchia[7], Wayne A Marasco[8,9], Zhengli-Li Shi[4] & Ralph S Baric[1,2]

The emergence of severe acute respiratory syndrome coronavirus (SARS-CoV) and Middle East respiratory syndrome (MERS)-CoV underscores the threat of cross-species transmission events leading to outbreaks in humans. Here we examine the disease potential of a SARS-like virus, SHC014-CoV, which is currently circulating in Chinese horseshoe bat populations[1]. Using the SARS-CoV reverse genetics system[2], we generated and characterized a chimeric virus expressing the spike of bat coronavirus SHC014 in a mouse-adapted SARS-CoV backbone. The results indicate that group 2b viruses encoding the SHC014 spike in a wild-type backbone can efficiently use multiple orthologs of the SARS receptor human angiotensin converting enzyme II (ACE2), replicate efficiently in primary human airway cells and achieve *in vitro* titers equivalent to epidemic strains of SARS-CoV. Additionally, *in vivo* experiments demonstrate replication of the chimeric virus in mouse lung with notable pathogenesis. Evaluation of available SARS-based immune-therapeutic and prophylactic modalities revealed poor efficacy; both monoclonal antibody and vaccine approaches failed to neutralize and protect from infection with CoVs using the novel spike protein. On the basis of these findings, we synthetically re-derived an infectious full-length SHC014 recombinant virus and demonstrate robust viral replication both *in vitro* and *in vivo*. Our work suggests a potential risk of SARS-CoV re-emergence from viruses currently circulating in bat populations.

The emergence of SARS-CoV heralded a new era in the cross-species transmission of severe respiratory illness with globalization leading to rapid spread around the world and massive economic impact[3,4]. Since then, several strains—including influenza A strains H5N1, H1N1 and H7N9 and MERS-CoV—have emerged from animal populations, causing considerable disease, mortality and economic hardship for the afflicted regions[5]. Although public health measures were able to stop the SARS-CoV outbreak[4], recent metagenomics studies have identified sequences of closely related SARS-like viruses circulating in Chinese bat populations that may pose a future threat[1,6]. However, sequence data alone provides minimal insights to identify and prepare for future prepandemic viruses. Therefore, to examine the emergence potential (that is, the potential to infect humans) of circulating bat CoVs, we built a chimeric virus encoding a novel, zoonotic CoV spike protein—from the RsSHC014-CoV sequence that was isolated from Chinese horseshoe bats[1]—in the context of the SARS-CoV mouse-adapted backbone. The hybrid virus allowed us to evaluate the ability of the novel spike protein to cause disease independently of other necessary adaptive mutations in its natural backbone. Using this approach, we characterized CoV infection mediated by the SHC014 spike protein in primary human airway cells and *in vivo*, and tested the efficacy of available immune therapeutics against SHC014-CoV. Together, the strategy translates metagenomics data to help predict and prepare for future emergent viruses.

The sequences of SHC014 and the related RsWIV1-CoV show that these CoVs are the closest relatives to the epidemic SARS-CoV strains (**Fig. 1a**,**b**); however, there are important differences in the 14 residues that bind human ACE2, the receptor for SARS-CoV, including the five that are critical for host range: Y442, L472, N479, T487 and Y491 (ref. 7). In WIV1, three of these residues vary from the epidemic SARS-CoV Urbani strain, but they were not expected to alter binding to ACE2 (**Supplementary Fig. 1a**,**b** and **Supplementary Table 1**). This fact is confirmed by both pseudotyping experiments that measured the ability of lentiviruses encoding WIV1 spike proteins to enter cells expressing human ACE2 (**Supplementary Fig. 1**) and by *in vitro* replication assays of WIV1-CoV (ref. 1). In contrast, 7 of 14 ACE2-interaction residues in SHC014 are different from those in SARS-CoV, including all five residues critical for host range (**Supplementary Fig. 1c** and **Supplementary Table 1**). These changes, coupled with

[1]Department of Epidemiology, University of North Carolina at Chapel Hill, Chapel Hill, North Carolina, USA. [2]Department of Microbiology and Immunology, University of North Carolina at Chapel Hill, Chapel Hill, North Carolina, USA. [3]National Center for Toxicological Research, Food and Drug Administration, Jefferson, Arkansas, USA. [4]Key Laboratory of Special Pathogens and Biosafety, Wuhan Institute of Virology, Chinese Academy of Sciences, Wuhan, China. [5]Department of Cell Biology and Physiology, University of North Carolina at Chapel Hill, Chapel Hill, North Carolina, USA. [6]Cystic Fibrosis Center, Marsico Lung Institute, University of North Carolina at Chapel Hill, Chapel Hill, North Carolina, USA. [7]Institute for Research in Biomedicine, Bellinzona Institute of Microbiology, Zurich, Switzerland. [8]Department of Cancer Immunology and AIDS, Dana-Farber Cancer Institute, Harvard Medical School, Boston, Massachusetts, USA. [9]Department of Medicine, Harvard Medical School, Boston, Massachusetts, USA. Correspondence should be addressed to R.S.B. (rbaric@email.unc.edu) or V.D.M. (vineet@email.unc.edu).

Received 12 June; accepted 8 October; published online 9 November 2015; corrected online 20 November 2015 (details online); doi:10.1038/nm.3985

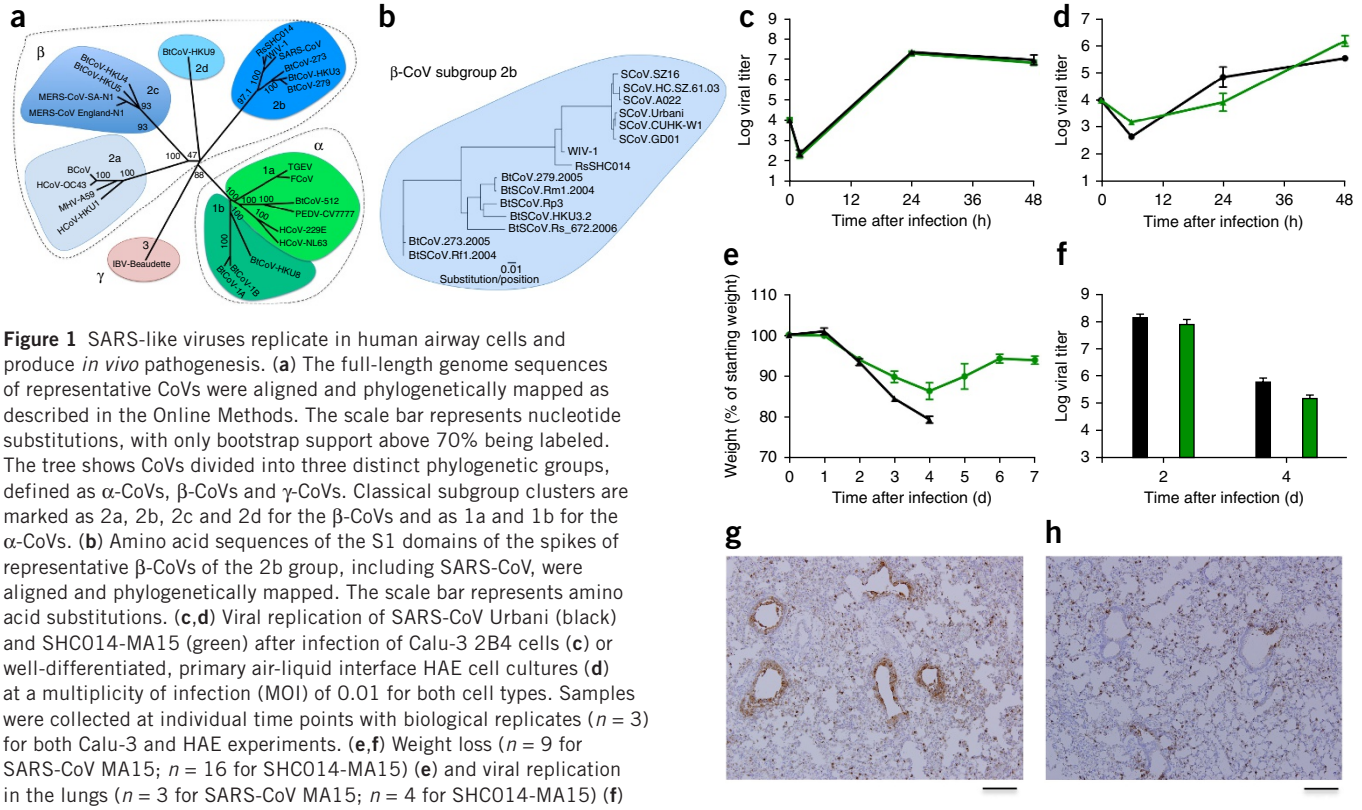

Figure 1 SARS-like viruses replicate in human airway cells and produce *in vivo* pathogenesis. (**a**) The full-length genome sequences of representative CoVs were aligned and phylogenetically mapped as described in the Online Methods. The scale bar represents nucleotide substitutions, with only bootstrap support above 70% being labeled. The tree shows CoVs divided into three distinct phylogenetic groups, defined as α-CoVs, β-CoVs and γ-CoVs. Classical subgroup clusters are marked as 2a, 2b, 2c and 2d for the β-CoVs and as 1a and 1b for the α-CoVs. (**b**) Amino acid sequences of the S1 domains of the spikes of representative β-CoVs of the 2b group, including SARS-CoV, were aligned and phylogenetically mapped. The scale bar represents amino acid substitutions. (**c**,**d**) Viral replication of SARS-CoV Urbani (black) and SHC014-MA15 (green) after infection of Calu-3 2B4 cells (**c**) or well-differentiated, primary air-liquid interface HAE cell cultures (**d**) at a multiplicity of infection (MOI) of 0.01 for both cell types. Samples were collected at individual time points with biological replicates ($n = 3$) for both Calu-3 and HAE experiments. (**e**,**f**) Weight loss ($n = 9$ for SARS-CoV MA15; $n = 16$ for SHC014-MA15) (**e**) and viral replication in the lungs ($n = 3$ for SARS-CoV MA15; $n = 4$ for SHC014-MA15) (**f**) of 10-week-old BALB/c mice infected with 1×10^4 p.f.u. of mouse-adapted SARS-CoV MA15 (black) or SHC014-MA15 (green) via the intranasal (i.n.) route. (**g**,**h**) Representative images of lung sections stained for SARS-CoV N antigen from mice infected with SARS-CoV MA15 ($n = 3$ mice) (**g**) or SHC014-MA15 ($n = 4$ mice) (**h**) are shown. For each graph, the center value represents the group mean, and the error bars define the s.e.m. Scale bars, 1 mm.

the failure of pseudotyped lentiviruses expressing the SHC014 spike to enter cells (**Supplementary Fig. 1d**), suggested that the SHC014 spike is unable to bind human ACE2. However, similar changes in related SARS-CoV strains had been reported to allow ACE2 binding[7,8], suggesting that additional functional testing was required for verification. Therefore, we synthesized the SHC014 spike in the context of the replication-competent, mouse-adapted SARS-CoV backbone (we hereafter refer to the chimeric CoV as SHC014-MA15) to maximize the opportunity for pathogenesis and vaccine studies in mice (**Supplementary Fig. 2a**). Despite predictions from both structure-based modeling and pseudotyping experiments, SHC014-MA15 was viable and replicated to high titers in Vero cells (**Supplementary Fig. 2b**). Similarly to SARS, SHC014-MA15 also required a functional ACE2 molecule for entry and could use human, civet and bat ACE2 orthologs (**Supplementary Fig. 2c**,**d**). To test the ability of the SHC014 spike to mediate infection of the human airway, we examined the sensitivity of the human epithelial airway cell line Calu-3 2B4 (ref. 9) to infection and found robust SHC014-MA15 replication, comparable to that of SARS-CoV Urbani (**Fig. 1c**). To extend these findings, primary human airway epithelial (HAE) cultures were infected and showed robust replication of both viruses (**Fig. 1d**). Together, the data confirm the ability of viruses with the SHC014 spike to infect human airway cells and underscore the potential threat of cross-species transmission of SHC014-CoV.

To evaluate the role of the SHC014 spike in mediating infection *in vivo*, we infected 10-week-old BALB/c mice with 10^4 plaque-forming units (p.f.u.) of either SARS-MA15 or SHC014-MA15 (**Fig. 1e**–**h**). Animals infected with SARS-MA15 experienced rapid weight loss and lethality by 4 d post infection (d.p.i.); in contrast, SHC014-MA15 infection produced substantial weight loss (10%) but no lethality in mice (**Fig. 1e**). Examination of viral replication revealed nearly equivalent viral titers from the lungs of mice infected with SARS-MA15 or SHC014-MA15 (**Fig. 1f**). Whereas lungs from the SARS-MA15–infected mice showed robust staining in both the terminal bronchioles and the lung parenchyma 2 d.p.i. (**Fig. 1g**), those of SHC014-MA15–infected mice showed reduced airway antigen staining (**Fig. 1h**); in contrast, no deficit in antigen staining was observed in the parenchyma or in the overall histology scoring, suggesting differential infection of lung tissue for SHC014-MA15 (**Supplementary Table 2**). We next analyzed infection in more susceptible, aged (12-month-old) animals. SARS-MA15–infected animals rapidly lost weight and succumbed to infection (**Supplementary Fig. 3a**,**b**). SHC014-MA15 infection induced robust and sustained weight loss, but had minimal lethality. Trends in the histology and antigen staining patterns that we observed in young mice were conserved in the older animals (**Supplementary Table 3**). We excluded the possibility that SHC014-MA15 was mediating infection through an alternative receptor on the basis of experiments using *Ace2*$^{-/-}$ mice, which did not show weight loss or antigen staining after SHC014-MA15 infection (**Supplementary Fig. 4a**,**b** and **Supplementary Table 2**). Together, the data indicate that viruses with the SHC014 spike are capable of inducing weight loss in mice in the context of a virulent CoV backbone.

Given the preclinical efficacy of Ebola monoclonal antibody therapies, such as ZMApp[10], we next sought to determine the efficacy of SARS-CoV monoclonal antibodies against infection with

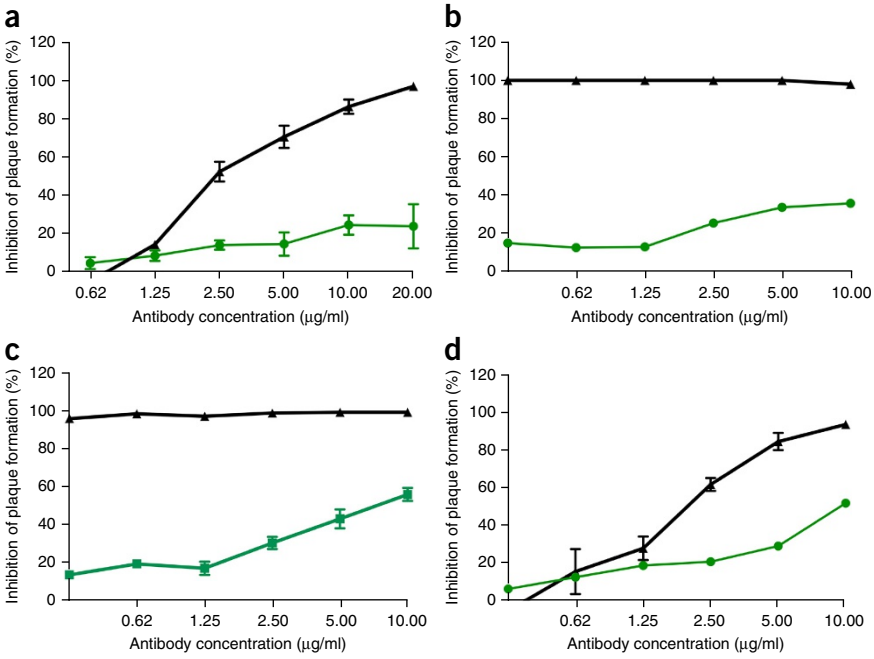

Figure 2 SARS-CoV monoclonal antibodies have marginal efficacy against SARS-like CoVs. (**a**–**d**) Neutralization assays evaluating efficacy (measured as reduction in the number of plaques) of a panel of monoclonal antibodies, which were all originally generated against epidemic SARS-CoV, against infection of Vero cells with SARS-CoV Urbani (black) or SHC014-MA15 (green). The antibodies tested were fm6 ($n = 3$ for Urbani; $n = 5$ for SHC014-MA15)[11,12] (**a**), 230.15 ($n = 3$ for Urbani; $n = 2$ for SHC014-MA15) (**b**), 227.15 ($n = 3$ for Urbani; $n = 5$ for SHC014-MA15) (**c**) and 109.8 ($n = 3$ for Urbani; $n = 2$ for SHC014-MA15)[13] (**d**). Each data point represents the group mean and error bars define the s.e.m. Note that the error bars in SARS-CoV Urbani–infected Vero cells in **b**,**c** are overlapped by the symbols and are not visible.

SHC014-MA15. Four broadly neutralizing human monoclonal antibodies targeting SARS-CoV spike protein had been previously reported and are probable reagents for immunotherapy[11–13]. We examined the effect of these antibodies on viral replication (expressed as percentage inhibition of viral replication) and found that whereas wild-type SARS-CoV Urbani was strongly neutralized by all four antibodies at relatively low antibody concentrations (**Fig. 2a–d**), neutralization varied for SHC014-MA15. Fm6, an antibody generated by phage display and escape mutants[11,12], achieved only background levels of inhibition of SHC014-MA15 replication (**Fig. 2a**). Similarly, antibodies 230.15 and 227.14, which were derived from memory B cells of SARS-CoV–infected patients[13], also failed to block SHC014-MA15 replication (**Fig. 2b**,**c**). For all three antibodies, differences between the SARS and SHC014 spike amino acid sequences corresponded to direct or adjacent residue changes found in SARS-CoV escape mutants (fm6 N479R; 230.15 L443V; 227.14 K390Q/E), which probably explains the absence of the antibodies' neutralizing activity against SHC014. Finally, monoclonal antibody 109.8 was able to achieve 50% neutralization of SHC014-MA15, but only at high concentrations (10 μg/ml) (**Fig. 2d**). Together, the results demonstrate that broadly neutralizing antibodies against SARS-CoV may only have marginal efficacy against emergent SARS-like CoV strains such as SHC014.

To evaluate the efficacy of existing vaccines against infection with SHC014-MA15, we vaccinated aged mice with double-inactivated whole SARS-CoV (DIV). Previous work showed that DIV could neutralize and protect young mice from challenge with a homologous virus[14]; however, the vaccine failed to protect aged animals in which augmented immune pathology was also observed, indicating the possibility of the animals being harmed because of the vaccination[15]. Here we found that DIV did not provide protection from challenge with SHC014-MA15 with regards to weight loss or viral titer (**Supplementary Fig. 5a**,**b**). Consistent with a previous report with other heterologous group 2b CoVs[15], serum from DIV-vaccinated, aged mice also failed to neutralize SHC014-MA15 (**Supplementary Fig. 5c**). Notably, DIV vaccination resulted in robust immune pathology (**Supplementary Table 4**) and eosinophilia (**Supplementary Fig. 5d–f**). Together, these results confirm that the DIV vaccine would not be protective against infection with SHC014 and could possibly augment disease in the aged vaccinated group.

In contrast to vaccination of mice with DIV, the use of SHC014-MA15 as a live, attenuated vaccine showed potential cross-protection against challenge with SARS-CoV, but the results have important caveats. We infected young mice with 10^4 p.f.u. of SHC014-MA15 and observed them for 28 d. We then challenged the mice with SARS-MA15 at day 29 (**Supplementary Fig. 6a**). The prior infection of the mice with the high dose of SHC014-MA15 conferred protection against challenge with a lethal dose of SARS-MA15, although there was only a minimal SARS-CoV neutralization response from the antisera elicited 28 d after SHC014-MA15 infection (**Supplementary Fig. 6b**, 1:200). In the absence of a secondary antigen boost, 28 d.p.i. represents the expected peak of antibody titers and implies that there will be diminished protection against SARS-CoV over time[16,17]. Similar results showing protection against challenge with a lethal dose of SARS-CoV were observed in aged BALB/c mice with respect to weight loss and viral replication (**Supplementary Fig. 6c**,**d**). However, the SHC014-MA15 infection dose of 10^4 p.f.u. induced >10% weight loss and lethality in some aged animals (**Fig. 1** and **Supplementary Fig. 3**). We found that vaccination with a lower dose of SHC014-MA15 (100 p.f.u.), did not induce weight loss, but it also failed to protect aged animals from a SARS-MA15 lethal dose challenge (**Supplementary Fig. 6e**,**f**). Together, the data suggest that SHC014-MA15 challenge may confer cross-protection against SARS-CoV through conserved epitopes, but the required dose induces pathogenesis and precludes use as an attenuated vaccine.

Having established that the SHC014 spike has the ability to mediate infection of human cells and cause disease in mice, we next synthesized a full-length SHC014-CoV infectious clone based on the approach used for SARS-CoV (**Fig. 3a**)[2]. Replication in Vero cells revealed no deficit for SHC014-CoV relative to that for SARS-CoV (**Fig. 3b**); however, SHC014-CoV was significantly ($P < 0.01$) attenuated in primary HAE cultures at both 24 and 48 h after infection (**Fig. 3c**). *In vivo* infection of mice demonstrated no significant weight loss but showed reduced viral replication in lungs of full-length SHC014-CoV infection, as compared to SARS-CoV Urbani (**Fig. 3d**,**e**). Together, the results establish the viability of full-length

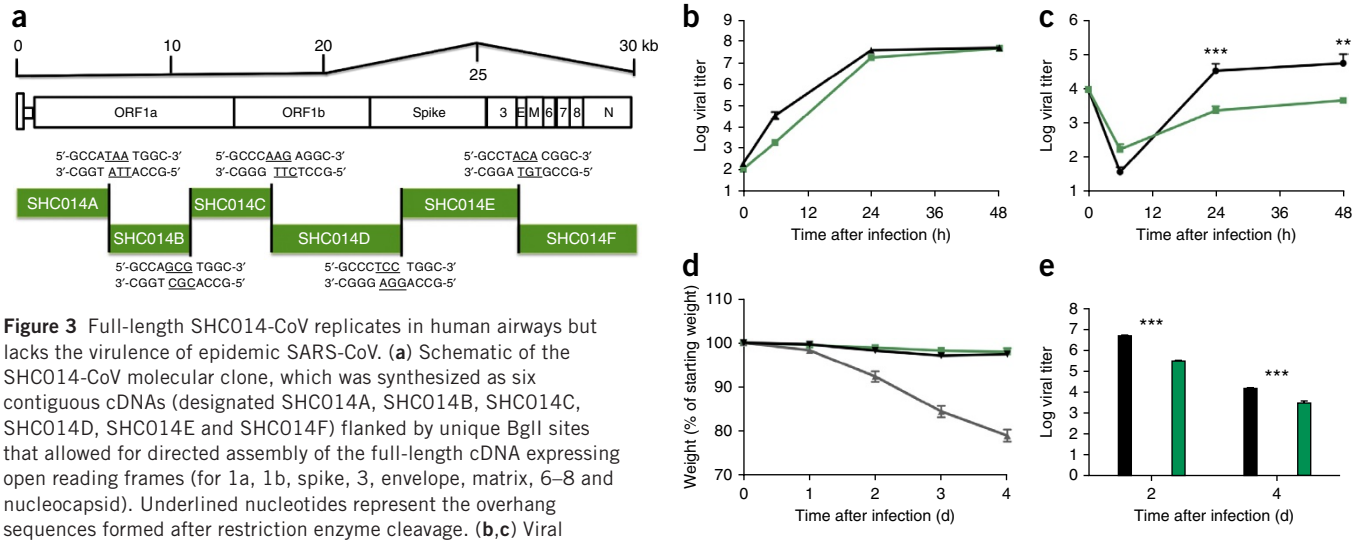

Figure 3 Full-length SHC014-CoV replicates in human airways but lacks the virulence of epidemic SARS-CoV. (**a**) Schematic of the SHC014-CoV molecular clone, which was synthesized as six contiguous cDNAs (designated SHC014A, SHC014B, SHC014C, SHC014D, SHC014E and SHC014F) flanked by unique BglI sites that allowed for directed assembly of the full-length cDNA expressing open reading frames (for 1a, 1b, spike, 3, envelope, matrix, 6–8 and nucleocapsid). Underlined nucleotides represent the overhang sequences formed after restriction enzyme cleavage. (**b**,**c**) Viral replication of SARS-CoV Urbani (black) or SHC014-CoV (green) after infection of Vero cells (**b**) or well-differentiated, primary air-liquid interface HAE cell cultures (**c**) at an MOI of 0.01. Samples were collected at individual time points with biological replicates ($n = 3$) for each group. Data represent one experiment for both Vero and HAE cells. (**d**,**e**) Weight loss ($n = 3$ for SARS-CoV MA15, $n = 7$ for SHC014-CoV; $n = 6$ for SARS-Urbani) (**d**) and viral replication in the lungs ($n = 3$ for SARS-Urbani and SHC014-CoV) (**e**) of 10-week-old BALB/c mice infected with 1×10^5 p.f.u. of SARS-CoV MA15 (gray), SHC014-CoV (green) or SARS-CoV Urbani (black) via the i.n. route. Each data point represents the group mean, and error bars define the s.e.m. $^{**}P < 0.01$ and $^{***}P < 0.001$ using two-tailed Student's *t*-test of individual time points.

SHC014-CoV, but suggest that further adaptation is required for its replication to be equivalent to that of epidemic SARS-CoV in human respiratory cells and in mice.

During the SARS-CoV epidemic, links were quickly established between palm civets and the CoV strains that were detected in humans[4]. Building on this finding, the common emergence paradigm argues that epidemic SARS-CoV originated as a bat virus, jumped to civets and incorporated changes within the receptor-binding domain (RBD) to improve binding to civet Ace2 (ref. 18). Subsequent exposure to people in live-animal markets permitted human infection with the civet strain, which, in turn, adapted to become the epidemic strain (**Fig. 4a**). However, phylogenetic analysis suggests that early human SARS strains appear more closely related to bat strains than to civet strains[18]. Therefore, a second paradigm argues that direct bat-human transmission initiated SARS-CoV emergence and that palm civets served as a secondary host and reservoir for continued infection (**Fig. 4b**)[19]. For both paradigms, spike adaptation in a secondary host is seen as a necessity, with most mutations expected to occur within the RBD, thereby facilitating improved infection. Both theories imply that pools of bat CoVs are limited and that host-range mutations are

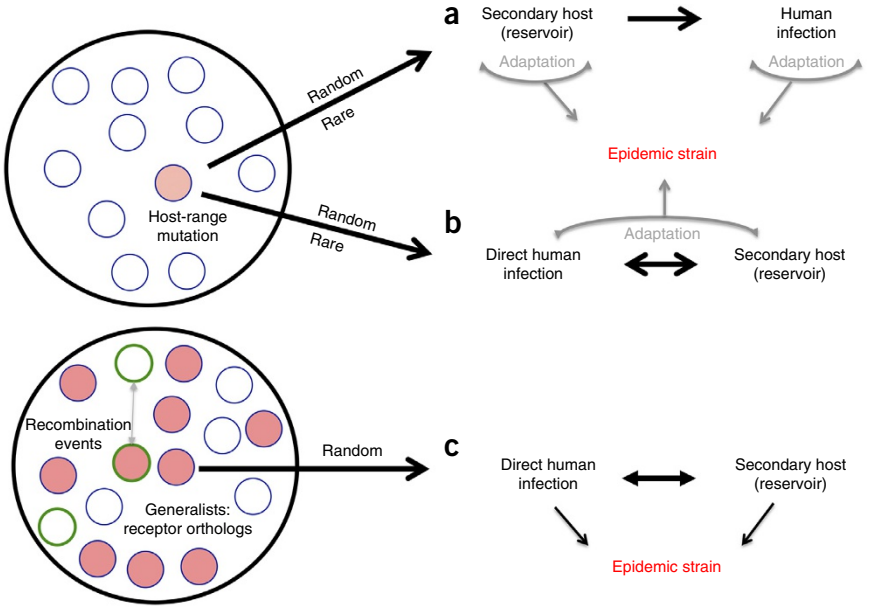

Figure 4 Emergence paradigms for coronaviruses. Coronavirus strains are maintained in quasi-species pools circulating in bat populations. (**a**,**b**) Traditional SARS-CoV emergence theories posit that host-range mutants (red circle) represent random and rare occurrences that permit infection of alternative hosts. The secondary-host paradigm (**a**) argues that a nonhuman host is infected by a bat progenitor virus and, through adaptation, facilitates transmission to humans; subsequent replication in humans leads to the epidemic viral strain. The direct paradigm (**b**) suggests that transmission occurs between bats and humans without the requirement of an intermediate host; selection then occurs in the human population with closely related viruses replicating in a secondary host, permitting continued viral persistence and adaptation in both. (**c**) The data from chimeric SARS-like viruses argue that the quasi-species pools maintain multiple viruses capable of infecting human cells without the need for mutations (red circles). Although adaptations in secondary or human hosts may be required for epidemic emergence, if SHC014 spike–containing viruses recombined with virulent CoV backbones (circles with green outlines), then epidemic disease may be the result in humans. Existing data support elements of all three paradigms.

both random and rare, reducing the likelihood of future emergence events in humans.

Although our study does not invalidate the other emergence routes, it does argue for a third paradigm in which circulating bat CoV pools maintain 'poised' spike proteins that are capable of infecting humans without mutation or adaptation (**Fig. 4c**). This hypothesis is illustrated by the ability of a chimeric virus containing the SHC014 spike in a SARS-CoV backbone to cause robust infection in both human airway cultures and in mice without RBD adaptation. Coupled with the observation of previously identified pathogenic CoV backbones[3,20], our results suggest that the starting materials required for SARS-like emergent strains are currently circulating in animal reservoirs. Notably, although full-length SHC014-CoV probably requires additional backbone adaption to mediate human disease, the documented high-frequency recombination events in CoV families underscores the possibility of future emergence and the need for further preparation.

To date, genomics screens of animal populations have primarily been used to identify novel viruses in outbreak settings[21]. The approach here extends these data sets to examine questions of viral emergence and therapeutic efficacy. We consider viruses with the SHC014 spike a potential threat owing to their ability to replicate in primary human airway cultures, the best available model for human disease. In addition, the observed pathogenesis in mice indicates a capacity for SHC014-containing viruses to cause disease in mammalian models, without RBD adaptation. Notably, differential tropism in the lung as compared to that with SARS-MA15 and attenuation of full-length SHC014-CoV in HAE cultures relative to SARS-CoV Urbani suggest that factors beyond ACE2 binding—including spike processivity, receptor bio-availability or antagonism of the host immune responses—may contribute to emergence. However, further testing in nonhuman primates is required to translate these finding into pathogenic potential in humans. Importantly, the failure of available therapeutics defines a critical need for further study and for the development of treatments. With this knowledge, surveillance programs, diagnostic reagents and effective treatments can be produced that are protective against the emergence of group 2b–specific CoVs, such as SHC014, and these can be applied to other CoV branches that maintain similarly heterogeneous pools.

In addition to offering preparation against future emerging viruses, this approach must be considered in the context of the US government–mandated pause on gain-of-function (GOF) studies[22]. On the basis of previous models of emergence (**Fig. 4a**,**b**), the creation of chimeric viruses such as SHC014-MA15 was not expected to increase pathogenicity. Although SHC014-MA15 is attenuated relative to its parental mouse-adapted SARS-CoV, similar studies examining the pathogenicity of CoVs with the wild-type Urbani spike within the MA15 backbone showed no weight loss in mice and reduced viral replication[23]. Thus, relative to the Urbani spike–MA15 CoV, SHC014-MA15 shows a gain in pathogenesis (**Fig. 1**). On the basis of these findings, scientific review panels may deem similar studies building chimeric viruses based on circulating strains too risky to pursue, as increased pathogenicity in mammalian models cannot be excluded. Coupled with restrictions on mouse-adapted strains and the development of monoclonal antibodies using escape mutants, research into CoV emergence and therapeutic efficacy may be severely limited moving forward. Together, these data and restrictions represent a crossroads of GOF research concerns; the potential to prepare for and mitigate future outbreaks must be weighed against the risk of creating more dangerous pathogens. In developing policies moving forward, it is important to consider the value of the data generated by these studies and whether these types of chimeric virus studies warrant further investigation versus the inherent risks involved.

Overall, our approach has used metagenomics data to identify a potential threat posed by the circulating bat SARS-like CoV SHC014. Because of the ability of chimeric SHC014 viruses to replicate in human airway cultures, cause pathogenesis *in vivo* and escape current therapeutics, there is a need for both surveillance and improved therapeutics against circulating SARS-like viruses. Our approach also unlocks the use of metagenomics data to predict viral emergence and to apply this knowledge in preparing to treat future emerging virus infections.

METHODS

Methods and any associated references are available in the online version of the paper.

Note: Any Supplementary Information and Source Data files are available in the online version of the paper.

ACKNOWLEDGMENTS

Research in this manuscript was supported by grants from the National Institute of Allergy & Infectious Disease and the National Institute of Aging of the US National Institutes of Health (NIH) under awards U19AI109761 (R.S.B.), U19AI107810 (R.S.B.), AI085524 (W.A.M.), F32AI102561 (V.D.M.) and K99AG049092 (V.D.M.), and by the National Natural Science Foundation of China awards 81290341 (Z.-L.S.) and 31470260 (X.-Y.G.), and by USAID-EPT-PREDICT funding from EcoHealth Alliance (Z.-L.S.). Human airway epithelial cultures were supported by the National Institute of Diabetes and Digestive and Kidney Disease of the NIH under award NIH DK065988 (S.H.R.). We also thank M.T. Ferris (Dept. of Genetics, University of North Carolina) for the reviewing of statistical approaches and C.T. Tseng (Dept. of Microbiology and Immunology, University of Texas Medical Branch) for providing Calu-3 cells. Experiments with the full-length and chimeric SHC014 recombinant viruses were initiated and performed before the GOF research funding pause and have since been reviewed and approved for continued study by the NIH. The content is solely the responsibility of the authors and does not necessarily represent the official views of the NIH.

AUTHOR CONTRIBUTIONS

V.D.M. designed, coordinated and performed experiments, completed analysis and wrote the manuscript. B.L.Y. designed the infectious clone and recovered chimeric viruses; S.A. completed neutralization assays; L.E.G. helped perform mouse experiments; T.S. and J.A.P. completed mouse experiments and plaque assays; X.-Y.G. performed pseudotyping experiments; K.D. generated structural figures and predictions; E.F.D. generated phylogenetic analysis; R.L.G. completed RNA analysis; S.H.R. provided primary HAE cultures; A.L. and W.A.M. provided critical monoclonal antibody reagents; and Z.-L.S. provided SHC014 spike sequences and plasmids. R.S.B. designed experiments and wrote manuscript.

COMPETING FINANCIAL INTERESTS

The authors declare no competing financial interests.

1. Ge, X.Y. *et al.* Isolation and characterization of a bat SARS-like coronavirus that uses the ACE2 receptor. *Nature* **503**, 535–538 (2013).
2. Yount, B. *et al.* Reverse genetics with a full-length infectious cDNA of severe acute respiratory syndrome coronavirus. *Proc. Natl. Acad. Sci. USA* **100**, 12995–13000 (2003).
3. Becker, M.M. *et al.* Synthetic recombinant bat SARS-like coronavirus is infectious in cultured cells and in mice. *Proc. Natl. Acad. Sci. USA* **105**, 19944–19949 (2008).
4. Peiris, J.S., Guan, Y. & Yuen, K.Y. Severe acute respiratory syndrome. *Nat. Med.* **10**, S88–S97 (2004).
5. Al-Tawfiq, J.A. *et al.* Surveillance for emerging respiratory viruses. *Lancet Infect. Dis.* **14**, 992–1000 (2014).
6. He, B. *et al.* Identification of diverse alphacoronaviruses and genomic characterization of a novel severe acute respiratory syndrome–like coronavirus from bats in China. *J. Virol.* **88**, 7070–7082 (2014).
7. Li, F. Receptor recognition and cross-species infections of SARS coronavirus. *Antiviral Res.* **100**, 246–254 (2013).

8. Sheahan, T. *et al.* Mechanisms of zoonotic severe acute respiratory syndrome coronavirus host range expansion in human airway epithelium. *J. Virol.* **82**, 2274–2285 (2008).
9. Yoshikawa, T. *et al.* Dynamic innate immune responses of human bronchial epithelial cells to severe acute respiratory syndrome–associated coronavirus infection. *PLoS ONE* **5**, e8729 (2010).
10. Qiu, X. *et al.* Reversion of advanced Ebola virus disease in nonhuman primates with ZMapp. *Nature* **514**, 47–53 (2014).
11. Sui, J. *et al.* Broadening of neutralization activity to directly block a dominant antibody-driven SARS-coronavirus evolution pathway. *PLoS Pathog.* **4**, e1000197 (2008).
12. Sui, J. *et al.* Effects of human anti–spike protein receptor binding domain antibodies on severe acute respiratory syndrome coronavirus neutralization escape and fitness. *J. Virol.* **88**, 13769–13780 (2014).
13. Rockx, B. *et al.* Escape from human monoclonal antibody neutralization affects *in vitro* and *in vivo* fitness of severe acute respiratory syndrome coronavirus. *J. Infect. Dis.* **201**, 946–955 (2010).
14. Spruth, M. *et al.* A double-inactivated whole-virus candidate SARS coronavirus vaccine stimulates neutralizing and protective antibody responses. *Vaccine* **24**, 652–661 (2006).
15. Bolles, M. *et al.* A double-inactivated severe acute respiratory syndrome coronavirus vaccine provides incomplete protection in mice and induces increased eosinophilic proinflammatory pulmonary response upon challenge. *J. Virol.* **85**, 12201–12215 (2011).
16. Siegrist, C.-A. in *Vaccines* 6th edn. (eds. Plotkin, S.A., Orenstein, W.A. & Offit, P.A.) 14–32 (W.B. Saunders, 2013).
17. Deming, D. *et al.* Vaccine efficacy in senescent mice challenged with recombinant SARS-CoV bearing epidemic and zoonotic spike variants. *PLoS Med.* **3**, e525 (2006).
18. Graham, R.L., Donaldson, E.F. & Baric, R.S. A decade after SARS: strategies for controlling emerging coronaviruses. *Nat. Rev. Microbiol.* **11**, 836–848 (2013).
19. Graham, R.L. & Baric, R.S. Recombination, reservoirs and the modular spike: mechanisms of coronavirus cross-species transmission. *J. Virol.* **84**, 3134–3146 (2010).
20. Agnihothram, S. *et al.* A mouse model for betacoronavirus subgroup 2c using a bat coronavirus strain HKU5 variant. *MBio* **5**, e00047-14 (2014).
21. Relman, D.A. Metagenomics, infectious disease diagnostics and outbreak investigations: sequence first, ask questions later? *J. Am. Med. Assoc.* **309**, 1531–1532 (2013).
22. Kaiser, J. Moratorium on risky virology studies leaves work at 14 institutions in limbo. *ScienceInsider* http://news.sciencemag.org/biology/2014/11/moratorium-risky-virology-studies-leaves-work-14-institutions-limbo (2014).
23. Frieman, M. *et al.* Molecular determinants of severe acute respiratory syndrome coronavirus pathogenesis and virulence in young and aged mouse models of human disease. *J. Virol.* **86**, 884–897 (2012).

ONLINE METHODS

Viruses, cells, *in vitro* infection and plaque assays. Wild-type SARS-CoV (Urbani), mouse-adapted SARS-CoV (MA15) and chimeric SARS-like CoVs were cultured on Vero E6 cells (obtained from United States Army Medical Research Institute of Infectious Diseases), grown in Dulbecco's modified Eagle's medium (DMEM) (Gibco, CA) and 5% fetal clone serum (FCS) (Hyclone, South Logan, UT) along with antibiotic/antimycotic (Gibco, Carlsbad, CA). DBT cells (Baric laboratory, source unknown) expressing *ACE2* orthologs have been previously described for both human and civet; bat *Ace2* sequence was based on that from *Rhinolophus leschenaulti*, and DBT cells expressing bat *Ace2* were established as described previously[8]. Pseudotyping experiments were similar to those using an HIV-based pseudovirus, prepared as previously described[10], and examined on HeLa cells (Wuhan Institute of Virology) that expressed *ACE2* orthologs. HeLa cells were grown in minimal essential medium (MEM) (Gibco, CA) supplemented with 10% FCS (Gibco, CA) as previously described[24]. Growth curves in Vero E6, DBT, Calu-3 2B4 and primary human airway epithelial cells were performed as previously described[8,25]. None of the working cell line stocks were authenticated or tested for mycoplasma recently, although the original seed stocks used to create the working stocks are free from contamination. Human lungs for HAE cultures were procured under University of North Carolina at Chapel Hill Institutional Review Board–approved protocols. HAE cultures represent highly differentiated human airway epithelium containing ciliated and non-ciliated epithelial cells as well as goblet cells. The cultures are also grown on an air-liquid interface for several weeks before use, as previously described[26]. Briefly, cells were washed with PBS and inoculated with virus or mock-diluted in PBS for 40 min at 37 °C. After inoculation, cells were washed three times and fresh medium was added to signify time '0'. Three or more biological replicates were harvested at each described time point. No blinding was used in any sample collections nor were samples randomized. All virus cultivation was performed in a biosafety level (BSL) 3 laboratory with redundant fans in the biosafety cabinets, as described previously by our group[2]. All personnel wore powered air purifying respirators (Breathe Easy, 3M) with Tyvek suits, aprons and booties and were double-gloved.

Sequence clustering and structural modeling. The full-length genomic sequences and the amino acid sequences of the S1 domains of the spike of representative CoVs were downloaded from Genbank or Pathosystems Resource Integration Center (PATRIC), aligned with ClustalX and phylogenetically compared by using maximum likelihood estimation using 100 bootstraps or by using the PhyML (https://code.google.com/p/phyml/) package, respectively. The tree was generated using maximum likelihood with the PhyML package. The scale bar represents nucleotide substitutions. Only nodes with bootstrap support above 70% are labeled. The tree shows that CoVs are divided into three distinct phylogenetic groups defined as α-CoVs, β-CoVs and γ-CoVs. Classical subgroup clusters are marked as 2a, 2b, 2c and 2d for β-CoVs, and 1a and 1b for the α-CoVs. Structural models were generated using Modeller (Max Planck Institute Bioinformatics Toolkit) to generate homology models for SHC014 and Rs3367 of the SARS RBD in complex with ACE2 based on crystal structure 2AJF (Protein Data Bank). Homology models were visualized and manipulated in MacPyMol (version 1.3).

Construction of SARS-like chimeric viruses. Both wild-type and chimeric viruses were derived from either SARS-CoV Urbani or the corresponding mouse-adapted (SARS-CoV MA15) infectious clone (ic) as previously described[27]. Plasmids containing spike sequences for SHC014 were extracted by restriction digest and ligated into the E and F plasmid of the MA15 infectious clone. The clone was designed and purchased from Bio Basic as six contiguous cDNAs using published sequences flanked by unique class II restriction endonuclease sites (BglI). Thereafter, plasmids containing wild-type, chimeric SARS-CoV and SHC014-CoV genome fragments were amplified, excised, ligated and purified. *In vitro* transcription reactions were then preformed to synthesize full-length genomic RNA, which was transfected into Vero E6 cells as previously described[2]. The medium from transfected cells was harvested and served as seed stocks for subsequent experiments. Chimeric and full-length viruses were confirmed by sequence analysis before use in these studies. Synthetic construction of chimeric mutant and full-length SHC014-CoV was approved by the University of North Carolina Institutional Biosafety Committee and the Dual Use Research of Concern committee.

Ethics statement. This study was carried out in accordance with the recommendations for the care and use of animals by the Office of Laboratory Animal Welfare (OLAW), NIH. The Institutional Animal Care and Use Committee (IACUC) of The University of North Carolina at Chapel Hill (UNC, Permit Number A-3410-01) approved the animal study protocol (IACUC #13-033) used in these studies.

Mice and *in vivo* infection. Female, 10-week-old and 12-month-old BALB/cAnNHsD mice were ordered from Harlan Laboratories. Mouse infections were done as previously described[20]. Briefly, animals were brought into a BSL3 laboratory and allowed to acclimate for 1 week before infection. For infection and live-attenuated virus vaccination, mice were anesthetized with a mixture of ketamine and xylazine and infected intranasally, when challenged, with 50 µl of phosphate-buffered saline (PBS) or diluted virus with three or four mice per time point, per infection group per dose as described in the figure legends. For individual mice, notations for infection including failure to inhale the entire dose, bubbling of inoculum from the nose, or infection through the mouth may have led to exclusion of mouse data at the discretion of the researcher; post-infection, no other pre-established exclusion or inclusion criteria are defined. No blinding was used in any animal experiments, and animals were not randomized. For vaccination, young and aged mice were vaccinated by footpad injection with a 20-µl volume of either 0.2 µg of double-inactivated SARS-CoV vaccine with alum or mock PBS; mice were then boosted with the same regimen 22 d later and challenged 21 d thereafter. For all groups, as per protocol, animals were monitored daily for clinical signs of disease (hunching, ruffled fur and reduced activity) for the duration of the experiment. Weight loss was monitored daily for the first 7 d, after which weight monitoring continued until the animals recovered to their initial starting weight or displayed weight gain continuously for 3 d. All mice that lost greater than 20% of their starting body weight were ground-fed and further monitored multiple times per day as long as they were under the 20% cutoff. Mice that lost greater than 30% of their starting body weight were immediately sacrificed as per protocol. Any mouse deemed to be moribund or unlikely to recover was also humanely sacrificed at the discretion of the researcher. Euthanasia was performed using an isoflurane overdose and death was confirmed by cervical dislocation. All mouse studies were performed at the University of North Carolina (Animal Welfare Assurance #A3410-01) using protocols approved by the UNC Institutional Animal Care and Use Committee (IACUC).

Histological analysis. The left lung was removed and submerged in 10% buffered formalin (Fisher) without inflation for 1 week. Tissues were embedded in paraffin and 5-µm sections were prepared by the UNC Lineberger Comprehensive Cancer Center histopathology core facility. To determine the extent of antigen staining, sections were stained for viral antigen using a commercially available polyclonal SARS-CoV anti-nucleocapsid antibody (Imgenex) and scored in a blinded manner by for staining of the airway and parenchyma as previously described[20]. Images were captured using an Olympus BX41 microscope with an Olympus DP71 camera.

Virus neutralization assays. Plaque reduction neutralization titer assays were performed with previously characterized antibodies against SARS-CoV, as previously described[11–13]. Briefly, neutralizing antibodies or serum was serially diluted twofold and incubated with 100 p.f.u. of the different infectious clone SARS-CoV strains for 1 h at 37 °C. The virus and antibodies were then added to a 6-well plate with 5×10^5 Vero E6 cells/well with multiple replicates ($n \geq 2$). After a 1-h incubation at 37 °C, cells were overlaid with 3 ml of 0.8% agarose in medium. Plates were incubated for 2 d at 37 °C, stained with neutral red for 3 h and plaques were counted. The percentage of plaque reduction was calculated as (1 − (no. of plaques with antibody/no. of plaques without antibody)) × 100.

doi:10.1038/nm.3985

Corrigendum: Multiphoton imaging reveals a new leukocyte recruitment paradigm in the glomerulus

Sapna Devi, Anqi Li, Clare L V Westhorpe, Camden Y Lo, Latasha D Abeynaike, Sarah L Snelgrove, Pam Hall, Joshua D Ooi, Christopher G Sobey, A Richard Kitching & Michael J Hickey
***Nat. Med.* 19, 107–112 (2013); published online 16 December 2012; corrected after print 12 August 2015**

In the published article, in the Online Methods section, it is stated that the dose of DHE used is 20 mg/kg, when in fact DHE was administered at 2 mg/kg. The error has been corrected in the HTML and PDF versions of the article.

Corrigendum: PAR1 signaling regulates the retention and recruitment of EPCR-expressing bone marrow hematopoietic stem cells

Shiri Gur-Cohen, Tomer Itkin, Sagarika Chakrabarty, Claudine Graf, Orit Kollet, Aya Ludin, Karin Golan, Alexander Kalinkovich, Guy Ledergor, Eitan Wong, Elisabeth Niemeyer, Ziv Porat, Ayelet Erez, Irit Sagi, Charles T Esmon, Wolfram Ruf & Tsvee Lapidot
***Nat. Med.* 21, 1307–1317 (2015); published online 12 October 2015; corrected after print 18 November 2015**

In the version of this article initially published, the first author's name was incorrect. The error has been corrected in the HTML and PDF versions of the article.

Corrigendum: Myeloid-derived growth factor (C19orf10) mediates cardiac repair following myocardial infarction

Mortimer Korf-Klingebiel, Marc R Reboll, Stefanie Klede, Torben Brod, Andreas Pich, Felix Polten, L Christian Napp, Johann Bauersachs, Arnold Ganser, Eva Brinkmann, Ines Reimann, Tibor Kempf, Hans W Niessen, Jacques Mizrahi, Hans-Joachim Schönfeld, Antonio Iglesias, Maria Bobadilla, Yong Wang & Kai C Wollert
***Nat. Med.* 21, 140–149 (2015); published online 12 January 2015; corrected after print 19 November 2015**

In the version of this article initially published, the article number in reference 13 is incorrectly stated as '100ra190' and should be '100ra90'. The error has been corrected in the HTML and PDF versions of the article.

Corrigendum: A SARS-like cluster of circulating bat coronaviruses shows potential for human emergence

Vineet D Menachery, Boyd L Yount Jr, Kari Debbink, Sudhakar Agnihothram, Lisa E Gralinski, Jessica A Plante, Rachel L Graham, Trevor Scobey, Xing-Yi Ge, Eric F Donaldson, Scott H Randell, Antonio Lanzavecchia, Wayne A Marasco, Zhengli-Li Shi & Ralph S Baric
***Nat. Med.*; doi:10.1038/nm.3985; corrected 20 November 2015**

In the version of this article initially published online, the authors omitted to acknowledge a funding source, USAID-EPT-PREDICT funding from EcoHealth Alliance, to Z.-L.S. The error has been corrected for the print, PDF and HTML versions of this article.

Corrigendum: Long-term glycemic control using polymer-encapsulated human stem cell–derived beta cells in immune-competent mice

Arturo J Vegas, Omid Veiseh, Mads Gürtler, Jeffrey R Millman, Felicia W Pagliuca, Andrew R Bader, Joshua C Doloff, Jie Li, Michael Chen, Karsten Olejnik, Hok Hei Tam, Siddharth Jhunjhunwala, Erin Langan, Stephanie Aresta-Dasilva, Srujan Gandham, James J McGarrigle, Matthew A Bochenek, Jennifer Hollister-Lock, Jose Oberholzer, Dale L Greiner, Gordon C Weir, Douglas A Melton, Robert Langer & Daniel G Anderson
***Nat. Med.*; doi:10.1038/nm.4030; corrected online 18 February 2016**

In the version of this article initially published online, the authors omitted acknowledgment recognizing the histology core of the Harvard Stem Cell Institute and several individuals for their assistance. The error has been corrected for the print, PDF and HTML versions of this article.